The Primordial Growth Disorder 3-M Syndrome Connects Ubiquitination to the Cytoskeletal Adaptor OBSL1

Dan Hanson,[1,2] Philip G. Murray,[1,2,3] Amit Sud,[1,2] Samia A. Temtamy,[4] Mona Aglan,[4] Andrea Superti-Furga,[5] Sue E. Holder,[6] Jill Urquhart,[2,3] Emma Hilton,[2] Forbes D.C. Manson,[2] Peter Scambler,[7] Graeme C.M. Black,[2,3,*] and Peter E. Clayton[1,3]

3-M syndrome is an autosomal-recessive primordial growth disorder characterized by significant intrauterine and postnatal growth restriction. Mutations in the *CUL7* gene are known to cause 3-M syndrome. In 3-M syndrome patients that do not carry *CUL7* mutations, we performed high-density genome-wide SNP mapping to identify a second locus at 2q35-q36.1. Further haplotype analysis revealed a 1.29 Mb interval in which the underlying gene is located and we subsequently discovered seven distinct null mutations from 10 families within the gene *OBSL1*. OBSL1 is a putative cytoskeletal adaptor protein that localizes to the nuclear envelope. We were also able to demonstrate that loss of OBSL1 leads to downregulation of CUL7, implying a role for OBSL1 in the maintenance of CUL7 protein levels and suggesting that both proteins are involved within the same molecular pathway.

3-M syndrome (MIM 273750) is characterized by prenatal growth restriction in the absence of recognizable maternal or placental pathology and by the failure of postnatal catch-up growth resulting in significant proportionate short stature. The syndrome is associated with distinct facial features (triangular face, flat maxillae, and prominent forehead), radiological abnormalities (tall vertebrae, slender long bones), and normal intelligence.[1–3] Final adult height is in the range of 115 to 150 cm (-4 to -8 SD[4]).

Pathogenic mutations in the *CUL7* gene (MIM 609577) cause 3-M syndrome including truncating, nonsense, and missense variants.[4–6] The protein product CUL7 is the most recently defined member of the Cullin family and is an integral part of the ubiquitin-proteasome pathway acting as a structural protein in the formation of a SCF-ROC1 complex. This consists of CUL7, SKP1, ROC1, and FBXW8 and functions as a multisubunit E3 ligase.[7] Although demonstrating that reduction or absence of CUL7 has a major impact on growth and cell division, the precise mechanisms by which this occurs remain unclear: CUL7 has an N-terminal binding domain for the tumor suppressor p53,[8] and microRNA knockdown leads to inhibition of cell cycle progression mediated by p53.[9] CUL7 also interacts with IRS-1, a downstream component of the signaling pathways of the insulin, IGF-I, and GH receptors. Mouse embryonic fibroblasts derived from *Cul7* knockout mice demonstrate accumulation of Irs-1, increased activation of Akt and Mapk pathways, and ultimately poor cellular growth and senescence.[10]

In the present study, we describe the mapping of a second locus for 3-M syndrome at 2q35-q36.1 and the subsequent identification of mutations in the *OBSL1* (MIM 610991) gene that encodes OBSL1, a putative cytoskeletal adaptor protein, suggesting that OBSL1 and CUL7 act in a common cellular pathway.

We identified 10 probands with the 3-M syndrome phenotype in whom direct DNA sequencing failed to detect *CUL7* mutations. All of the patients were phenotypically indistinguishable from those with *CUL7* mutations. Detailed clinical phenotype and auxology were available for eight of the patients. Clinical phenotype, growth, and radiological features are summarized in Table 1. All patients had a distinctive facial appearance with anteverted nares, fleshy tipped nose, frontal bossing, and midface hypoplasia (Figure 1). Prominent heels were present in all cases. In keeping with previous reports, our patients had low weight and height standard deviations scores (SDS) with a relatively preserved occipitofrontal circumference SDS. Height SDS toward the end of childhood was in the range of -3 to -5 SDS. There were no clear differences in phenotype between 3-M patients with *OBSL1* mutations and those previously reported with mutations in *CUL7*.

Two of the probands (3-M-4 and -5) were from multiple affected consanguineous kindreds comprising four and three affected individuals, respectively. Neither family exhibited linkage to the *CUL7* locus, indicating that 3-M syndrome displays locus heterogeneity. We hypothesized that identification of further causative genes might shed light on a shared biochemical pathway controlling mammalian growth. With this in mind, we conducted whole-genome-wide autozygosity mapping with 250 ng of genomic DNA with the HindIII array from the 100K Affymetrix GeneChip Human mapping set. Blood samples and informed consent were obtained from the affected individuals and unaffected relatives. This study was approved by our institution's research ethics committee and conducted with their ethical standards.

[1]Endocrine Sciences, Faculty of Medical & Human Sciences, University of Manchester, Manchester M13 9NT, UK; [2]Medical Genetics, Faculty of Medical & Human Sciences, University of Manchester, Manchester M13 9PT, UK; [3]Central Manchester University Hospitals Foundation Trust, Manchester M13 0JH, UK; [4]Department of Clinical Genetics, Division of Human Genetics & Human Genome Research, National Research Centre, 12311 Cairo, Egypt; [5]Centre for Pediatrics & Adolescent Medicine, University of Freiburg, 79106 Freiburg, Germany; [6]North West Thames Regional Genetics Service, North West London Hospitals NHS Trust, Harrow HA1 3UJ, UK; [7]Molecular Medicine Unit, Institute of Child Health, London WC1N 1EH, UK
*Correspondence: gblack@manchester.ac.uk

Table 1. Clinical Findings of 3-M Syndrome Patients

Auxology

3-M ID	2	3	4	5	6	8	9a	9b
Gender	F	F	F	M	M	F	M	M
Birth weight (g)	2409	1900	NA	1920	2100	NA	NA	NA
Birth weight SDS	−2.63	−1.96	NA	−3.86	−3.77	NA	NA	NA
Age initial presentation (years)	1.4	0.2	11.7	4.5	1.0	NA	13.0	11.0
Height SDS at presentation	−6.4	−1.4	−4.8	−7.9	−7.8	NA	−4.6	−3.3
Weight SDS at presentation	−4.1	−1.2	−4.9	−8.6	−8.6	NA	−1.7	−1.3
OFC SDS at presentation	+2.4	+1.9	NA	−3.60	−3.3	NA	−0.8	+0.9

Radiological Features

Tall vertebrae	+	-	+	-	-	+	-	-
Slender long bones	-	+	-	-	+	-	+	+

Facial Features

Fleshy tipped nose	+	+	+	+	+	+	+	+
Anteverted nares	+	+	+	+	+	+	+	+
Full fleshy lips	+	+	-	+	-	+	+	+
Triangular face	+	+	+	+	-	+	+	+
Dolicocephaly	+	+	+	-	+	+	+	+
Frontal bossing	+	+	+	+	+	+	+	+
Midface hypoplasia	+	+	+	+	+	+	+	+
Long philtrum	-	+	-	-	+	+	+	+
Pointed chin	+	-	+	+	+	+	+	+
Prominent ears	-	+	-	+	+	-	+	+

Other Clinical Features

Short neck	-	-	+	+	+	+	+	-
Winged scapulae	-	-	-	-	-	-	+	+
Square shoulders	-	-	+	+	+	-	+	+
Short thorax	-	+	-	+	+	-	+	+
Transverse chest groove	-	-	+	+	-	-	+	+
Pectus deformity	-	+	+	+	+	-	-	-
Hyperlordosis	+	+	+	+	+	-	+	+
Scoliosis	-	+	-	-	-	-	-	-
Hypermobility of joints	-	-	-	-	-	-	-	-
5th finger clinodactyly	-	-	-	+	-	-	+	+
Prominent heels	+	+	+	+	+	+	+	+
Spina bifida occulta	-	-	-	-	-	-	-	-

Auxology, radiological features, and clinical phenotype in eight children with 3-M syndrome resulting from mutations in OBSL1. List of clinical features taken from Temtamy et al.[3].

Genomic DNA was isolated from whole blood samples via QIAGEN DNeasy kit. The array consists of 57,244 SNP markers with a mean marker distance of 47.2 kb. SNP genotype analysis was conducted with the AutoSNPa program to detect regions of shared homozygosity.[11] The SNP genotype call rate achieved was 98.15%.

All four affected siblings from family 3-M-4 shared two regions of homozygosity (Chr2: 218,018,585–225,142, 689 bp and Chr14: 32,542,986–38,094,746 bp). Within the region on chromosome 2 (2q35-q36.1), a smaller critical region was also shared by all three affected individuals in family 3-M-5 and a proband from a further consanguineous family, 3-M-6. The refined locus for 3-M syndrome was a 5.7 Mb region flanked by recombinants at 218, 018,585 bp (rs966423) and 223,752,494 bp (rs1597167) (Figure 2A). The critical region contains 63 known and hypothetical genes, 3 known miRNAs, and 5 known pseudogenes. One of the 20 loci recently shown to be associated with adult height (SNP rs6724465) lies in this region close to Indian Hedgehog (IHH [MIM 600726]), which has been implicated in the control of human growth.[12] However, direct sequencing of IHH was undertaken for two affected probands and failed to identify a causative mutation.

After the initial screening for mutations in genes within the 5.7 Mb critical region, haplotype analysis among the probands homozygous for this region demonstrated a shared haplotype between SNPs rs1516086 and rs10498071 for families 3-M-4 and -5 as well as the affected proband from family 3-M-6 (Figure 2B). This region extends over 1.29 Mb (Chr2: 219,139,779–220,430,942 bp) and encodes for 43 known and hypothetical genes, 2 known miRNAs, and 4 known pseudogenes. A further family, 3-M-8, also demonstrated autozygosity but did not share the same haplotype
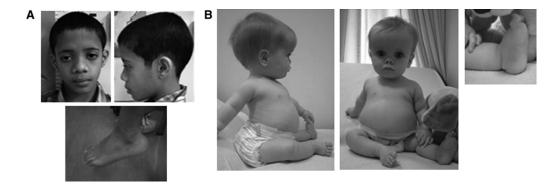
Figure 1. Clinical Features of 3-M Syndrome Patients
(A) A patient from family 3-M-6 aged 10 years. The facial appearance is characterized by fleshy tipped anteverted nares, full fleshy lips, triangular shaped face, midface hypoplasia, and prominent ears. These features become less prominent with increasing age.
(B) The affected child from family 3-M-2 aged 10 months. Facial appearance is characterized by similar fleshy tipped anteverted nares, full fleshy lips, triangular shaped face, and midface hypoplasia seen in 3-M-6 but also distinct frontal bossing. Both had proportionate short stature. Prominent heels are seen in most patients and may be a useful diagnostic feature. Patient photographs and X-rays from two brothers from family 3-M-9 have previously been reported by Temtamy et al.[3].

(Table 2). This suggested that the underlying mutation in families 3-M-4, -5, and -6 would differ from the mutation in 3-M-8.

Direct sequencing of genes in the 1.29 Mb critical region was undertaken for two affected probands. Pathogenic variants were identified in *OBSL1*, encoding the cytoskeletal linker protein obscurin-like 1 (Figures 2C and 2D). The *OBSL1* gene, identified via homology searches with obscurin, comprises 22 exons over a genomic region of 25 kb[13] with three splice forms which encode distinct isoforms (termed OBSL1 A, B, and C) with molecular masses of approximately 230, 130, and 170 kDa, respectively (Figure 2C).[13] Intronic primer pairs for each of the 22 exons of *OBSL1* were designed with Primer3 software.[14] Amplification of each fragment was conducted by standard PCR technique, and products were purified with Montage PCR filter units (Millipore) and sequenced with Applied Biosystems BDv3.1 on an ABI3730 automated analyzer (Applied Biosystems). Sequences were compared to both control genomic DNA and the published sequence (Ensembl ID ENSG00000124006, GenBank accession # NC_000002.10) with SeqScape software (Applied Biosystems).

In total, we identified 7 different *OBSL1* mutations in 18 patients from 10 families (Table 3) that are all presumptive null mutations. The mutations were not identified in a panel of 105 ethnically matched control samples, suggesting that the sequence variants are not common polymorphisms. All of the mutations identified in these families lie within the first 6 exons of the gene and thus affect all known isoforms.

We first assessed whether the *OBSL1* mutations identified induce nonsense-mediated decay (NMD) as predicted or would allow illegitimate downstream translation, explaining the clustering of mutations near to the N terminus of OBSL1. OBSL1 truncating mutants were created by PCR via an IMAGE: 2961284 cDNA clone containing the cDNA sequence that corresponds to OBSL1 isoform B (GenBank accession # BC007201). PCR products were cloned into pcDNA3.1 (Invitrogen) creating N-V5-OBSL1, C-V5-OBSL1, N-V5-OBSL1 c.1273insA, N-V5-OBSL1 c.1463C → T, C-V5-OBSL1 c.1273insA, and C-V5-OBSL1 c.1463C → T constructs. Each isoform was fused to a V5 tag at either the N or C termini. Both wild-type and mutant isoforms of a full-length human *OBSL1* cDNA (c.1273insA and c.1463C → T) were transiently expressed in HEK293 cells via Effectene transfection reagent (QIAGEN) according to the manufacturer's protocol. Protein expression was analyzed by standard western blot protocol with a monoclonal antibody for V5 (AbD Serotec). For both mutant isoforms, we were able to detect N-terminally tagged proteins but unable to detect C-terminally tagged proteins (Figure 3A). This suggested that no alternative translational start site would be used in the event of mutations located toward the N terminus of OBSL1. We therefore conclude that these mutations result in the loss of OBSL1, and given the phenotypic similarity in patients with *OBSL1* mutations, that 3-M syndrome represents the null phenotype of human OBSL1.

In order to assess the effects of *OBSL1* loss, we knocked it down by using two separate siRNAs in HEK293 cells (Figure 3B). Both siRNAs were designed to target all three isoforms of OBSL1 (Ambion) and were transfected into HEK293 cells with siPORT Amine transfection reagent (Ambion) according to the manufacturer's recommended protocol. 48 hr after transfection, cells were lysed followed by analysis of protein expression by western blot with a custom polyclonal antibody to OBSL1 (Eurogentec) and monoclonal antibodies for GAPDH, p53, and CUL7 (Santa-Cruz Biotechnology). We were unable to detect either OBSL1 or CUL7, suggesting a role for OBSL1 in the maintenance of normal levels of CUL7. In the same experiment, expression of p53
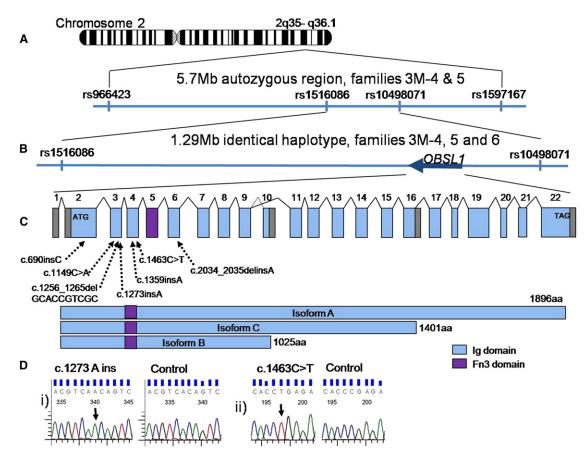
Figure 2. Genetic Mapping of the Second 3-M Syndrome Locus
(A) The region of common autozygosity shared between 3-M families 4 and 5 is located between rs966423 and rs1597167.
(B) The identical haplotype shared between 3-M families 4–6 located between rs1516086 and rs10498071.
(C) Exon and intron structure of OBSL1 with mutations identified in 10 3-M syndrome families and domain structure of each OBSL1 isoform.
(D) Sequence traces of the OBSL1 mutations (i. families 2–7; ii. family 9) with corresponding wild-type sequences.

was unchanged (Figure 3B) as has previously been shown in $Cul7^{-/-}$ MEFs in which p53 levels were also unchanged.[15]

To our knowledge we report the first identification of pathogenic sequence variants in *OBSL1,* a cytoskeletal adaptor protein, causing the primordial growth disorder 3-M syndrome. OBSL1 is homologous to obscurin, which is a muscle protein localized to sarcomeres implicated in cell signaling. Obscurin interacts with titin and myomesin, proteins involved in anchoring myosin filaments at the M-band in myocytes, and both titin and myomesin also interact with OBSL1.[16] Expression of *OBSL1* has been demonstrated in human heart and skeletal muscle,[13] a finding we have confirmed in the mouse, in which the strongest expression was demonstrated at stage E11.5 in the developing myotomes (data not shown).

OBSL1 consists entirely of immunoglobulin-like domains and a single fibronectin domain; this tertiary structure would suggest a primary role in protein-protein interaction. Geisler et al. postulated that this would be to stabilize the cytoskeletal network or act as a scaffold for signaling complexes with a proposal that disruption of OBSL1 would cause either skeletal or cardiac myopathy.[13] In our current investigation, however, patients with mutations in *OBSL1* were not found to have cardiovascular or muscular symptoms and it is possible that the overlapping ability of both OBSL1 and obscurin to bind titin and myomesin provides a degree of redundancy to explain this.

All mutations occurred in the first six exons of the *OBSL1* gene. We were able to demonstrate that all mutations reported do not induce nonsense-associated altered splicing (NAS), a mechanism by which alternatively spliced mRNA transcripts skipping the premature termination codon (PTC) are retained.[17] It is therefore likely that *OBSL1* mutations induce the NMD pathway. The NMD pathway is the opposite of the NAS pathway whereby mRNAs containing a PTC are rapidly degraded.[18] Therefore, the identification of a hot-spot is unexpected because mutations located in any coding exon except the last would induce the same NMD mechanism. We propose that mutations near the N terminus lead to loss of all OBSL1 isoforms, explaining the clustering of mutations in this region of the gene; we hypothesize that 3-M syndrome represents the

Table 2. Haplotype Analysis of Consanguineous 3-M Syndrome Families

Position	SNP ID	Allele A	Allele B	3-M-4	3-M-5	3-M-6	3-M-8
219139779	rs1516086	C	T	AA	AA	AA	AA
219220550	rs10498061	A	G	BB	BB	BB	BB
219228649	rs3931102	A	G	BB	BB	BB	BB
219245468	rs2241527	A	G	AA	AA	AA	AA
219246263	rs1344645	A	C	AA	AA	AA	AA
219247043	rs7604319	G	T	AA	AA	AA	AA
219309636	rs7573999	A	G	BB	BB	BB	BB
219529413	rs4672907	C	T	BB	BB	BB	AA
219668323	rs10498064	A	T	NoCall	BB	BB	BB
219711078	rs6436114	A	C	BB	BB	BB	BB
219719336	rs2293081	A	C	BB	BB	BB	AA
219720820	rs7585742	C	G	BB	BB	BB	AA
219757631	rs2385393	C	T	AA	AA	AA	AA
219874198	rs2292607	C	T	BB	BB	BB	BB
220249416	rs10498065	C	T	AA	AA	AA	BB
220287516	rs714132	A	T	BB	BB	BB	BB
220288529	rs2385573	A	G	BB	BB	BB	AA
220288792	rs678134	C	T	AA	AA	AA	AA
220368946	rs10498069	A	G	BB	BB	BB	BB
220380412	rs2113855	C	T	BB	BB	BB	BB
220430942	rs10498071	C	T	AA	AA	AA	AA

Haplotype analysis with identical genotypes in 3-M-4, -5, and -6 between rs1516086 and rs10498071, with 3-M-8 having an alternative haplotype.

null phenotype. The occurrence of a common mutation (p.T425NfsX40) in a large number of families from the same ethnic (Asian) background suggests that this may be a founder mutation, an observation supported by SNP analyses. Additionally, we have identified consanguineous families with 3-M syndrome who have neither *CUL7* nor *OBSL1* mutations and who are not linked to either genomic region, indicating that there is at least one further locus causing this growth disorder.

Because pathogenic *CUL7* mutations also cause 3-M syndrome, we proposed that OBSL1 acts within the same pathway as CUL7 or is involved in trafficking of the CUL7 SCF complex, a suggestion supported by the observation that knockdown of OBSL1 via siRNAs in HEK cells leads to concomitant knockdown of CUL7. Thus we suggest that loss of CUL7 either through mutations in CUL7 or through loss of OBSL1 may lead to a decrease in cell proliferation

resulting in the 3-M syndrome phenotype. This therefore implicates two hitherto unrelated cytoplasmic proteins in the pathogenesis of the human growth disorder 3-M syndrome, one a ubiquitin ligase (CUL7) and the other a cytoskeletal adaptor (OBSL1). The identification of the ubiquitinated target of the CUL7 SCF complex will likely further enhance our understanding of how defects in CUL7/OBSL1 pathway cause pre- and postnatal growth restriction. The characterization of disorders associated
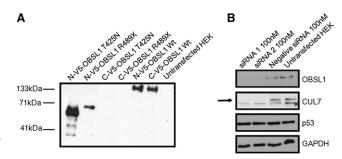
Table 3. Mutations Identified in *OBSL1*

3-M ID	Nucleotide Change	Protein Change
1	c.690insC	p.E231RfsX23
2	c.1149C → A; c.1273insA	p.C383X; p.T425NfsX40
3	c.1256_1265 delGCACCGTGGC; c.1273insA	p.R419PfsX10; p.T425NfsX40
4	c.1273insA	p.T425NfsX40
5	c.1273insA	p.T425NfsX40
6	c.1273insA	p.T425NfsX40
7	c.1273insA	p.T425NfsX40
8	c.1359insA	p.E454RfsX11
9	c.1463C → T	p.R489X
10	c.2034_2035 delinsA	p.H679TfsX40

OBSL1 mutations identified in 10 families with 3-M syndrome. Where a single mutation is listed, patients are homozygous for that mutation.

Figure 3. *OBSL1* Mutations Induce NMD and siRNA Knockdown of OBSL1 Results in Decreased CUL7 Expression

(A) Western blot analysis of V5-tagged OBSL1 clones. Expression of N- or C-terminally tagged *OBSL1* isoforms in HEK293 cells led to the detection of N-tagged isoforms (lanes 1 and 2) but not of C-tagged isoforms (lanes 3 and 4), demonstrating the expression of prematurely truncated isoforms. Wild-type protein tagged at either terminus was detected (lanes 5 and 6).

(B) siRNA knockdown of OBSL1 in HEK293 cells via two different siRNAs (that target all three wild-type isoforms) resulted in the decreased expression of CUL7 (second from top, upper band [arrow], lower band represents nonspecific binding) but did not alter the expression of p53 (third from top). The bottom gel shows a GAPDH loading control.

with significant pre- and postnatal growth retardation can allow identification of potential human growth regulators as demonstrated recently by the studies of primordial dwarfism (microcephalic osteodysplastic primordial dwarfism type II [MIM 210720]), demonstrating the importance to human growth of the mitotic spindle in regulating normal chromosome segregation.[19] We now demonstrate that the CUL7/OBSL1 pathway is also a key contributor to the regulation of human growth.

Supplemental Data

Supplemental Data include two tables and can be found with this article online at http://www.ajhg.org/.

Web Resources

The URLs for data presented herein are as follows:

AutoSNPa, http://dna.leeds.ac.uk/autosnpa/
Ensembl, http://www.ensembl.org/index.html
Online Mendelian Inheritance in Man (OMIM), http://www.ncbi.nlm.nih.gov/Omim/
Primer3, http://frodo.wi.mit.edu/

References

1. Miller, J.D., McKusick, V.A., Malvaux, P., Temtamy, S., and Salinas, C. (1975). The 3-M syndrome: A heritable low birth-weight dwarfism. Birth Defects Orig. Artic. Ser. *11*, 39–47.

2. Van der Wal, G., Otten, B.J., Brunner, H.G., and van der Burgt, I. (2001). 3-M syndrome: Description of six new patients with review of the literature. Clin. Dysmorphol. *10*, 241–252.

3. Temtamy, S.A., Aglan, M.S., Ashour, A.M., Ramzy, M.I., Hosny, L.A., and Mostafa, M.I. (2006). 3-M syndrome: A report of three Egyptian cases with review of the literature. Clin. Dysmorphol. *15*, 55–64.

4. Huber, C., Dias-Santagata, D., Glaser, A., O'Sullivan, J., Brauner, R., Wu, K., Xu, X., Pearce, K., Wang, R., Uzielli, M.L., et al. (2005). Identification of mutations in *CUL7* in 3-M syndrome. Nat. Genet. *37*, 1119–1124.

5. Maksimova, N., Hara, K., Miyashia, A., Nikolaeva, I., Shiga, A., Nogovicina, A., Sukhomyasova, A., Argunov, V., Shvedova, A., Ikeuchi, T., et al. (2007). Clinical, molecular and histopathological features of short stature syndrome with novel *CUL7* mutation in Yakuts: New population isolate in Asia. J. Med. Genet. *44*, 772–778.

6. Tsutsumi, T., Kuwabara, H., Arai, T., Xiao, Y., and Decaprio, J.A. (2008). Disruption of the *Fbxw8* gene results in pre- and postnatal growth retardation in mice. Mol. Cell. Biol. *28*, 743–751.

7. Dias, D.C., Dolios, G., Wang, R., and Pan, Z.Q. (2002). CUL7: A DOC domain-containing cullin selectively binds Skp1.Fbx29 to form an SCF-like complex. Proc. Natl. Acad. Sci. USA *99*, 16601–16606.

8. Andrews, P., He, Y.J., and Xiong, Y. (2006). Cytoplasmic localized ubiquitin ligase cullin 7 binds to p53 and promotes cell growth by antagonizing p53 function. Oncogene *25*, 4534–4548.

9. Jung, P., Verdoodt, B., Bailey, A., Yates, J.R. 3rd, Menssen, A., and Hermeking, H. (2007). Induction of cullin 7 by DNA damage attenuates p53 function. Proc. Natl. Acad. Sci. USA *104*, 11388–11393.

10. Xu, X., Sarikas, A., Dias-Santagata, D.C., Dolios, G., Lafontant, P.J., Tsai, S.C., Zhu, W., Nakajima, H., Nakajima, H.O., Field, L.J., et al. (2008). The CUL7 E3 ubiquitin ligase targets insulin receptor substrate 1 for ubiquitin-dependent degradation. Mol. Cell *23*, 403–414.

11. Carr, I.M., Flintoff, K., Taylor, G.R., Markham, A.F., and Bonthron, D.T. (2006). Interactive visual analysis of SNP data for rapid autozygosity mapping in consanguineous families. Hum. Mutat. *27*, 1041–1046.

12. Weedon, M.N., Lango, H., Lindgren, C.M., Wallace, C., Evans, D.M., Mangino, M., Freathy, R.M., Perry, J.R., Stevens, S., Hall, A.S., et al. (2008). Genome-wide association analysis identifies 20 loci that influence adult height. Nat. Genet. *40*, 575–583.

13. Geisler, S.B., Robinson, D., Hauringa, M., Raeker, M.O., Borisov, A.B., Westfall, M.V., and Russell, M.W. (2007). Obscurin-like 1, OBSL, is a novel cytoskeletal protein related to obscurin. Genomics *89*, 521–531.

14. Rozen, S., and Skaletsky, H. (2000). Primer3 on the WWW for general users and for biologist programmers. Methods Mol. Biol. *132*, 365–386.

15. Kasper, J.S., Arai, T., and DeCaprio, J.A. (2006). A novel p53-binding domain in CUL7. Biochem. Biophys. Res. Commun. *15*, 132–138.

16. Fukuzawa, A., Lange, S., Holt, M., Vihola, A., Carmignac, V., Ferreiro, A., Udd, B., and Gautel, M.J. (2008). Interactions with titin and myomesin target obscurin and obscurin-like 1 to the M-band: Implications for hereditary myopathies. Cell Sci. *121*, 1841–1851.

17. Wang, J., Chang, Y.-F., Hamilton, J.I., and Wilkinson, M.F. (2002). Nonsense-associated altered splicing: A frame dependent response distinct from nonsense-mediated decay. Mol. Cell *10*, 951–957.

18. Li, S., and Wilkinson, M.F. (1998). Nonsense surveillance in lymphocytes? Immunity *8*, 135–141.

19. Rauch, A., Thiel, C.T., Schindler, D., Wick, U., Crow, Y.J., Ekici, A.B., van Essen, A.J., Goecke, T.O., Al-Gazali, L., Chrzanowska, K.H., et al. (2008). Mutations in the pericentrin (*PCNT*) gene cause primordial dwarfism. Science *319*, 816–819.